

The Safe Basin Erosion of a Ship in Waves with Single Degree of Freedom

X. Wu¹, L. Tao¹ and Y. Li²

¹School of Engineering, Griffith University, PMB50 GCMC, QLD9726 AUSTRALIA

²Department of Naval Architecture & Marine Engineering, South China University of Technology, CHINA

Abstract

The safety of a ship is studied using the theory of "safe basin" in this paper. The safe basins of the single degree of freedom (rolling) in waves and winds are investigated. The influences of a static heel angle, waves and winds to the safe basin erosion are examined. It is found that the shape of the safe basin is changed when a static bias angle takes place, and the area of the safe basin decreases while the static heel angle increases, but the safe basin will begin to erode in waves or winds.

Introduction

Current practice in the stability design of ships is based on the righting lever in still water (the GZ curve). Such an approach considers a ship in calm water, and imposes certain restrictions on the characteristics of the GZ curve. As a measure of the safety of a ship, the GZ curve gives a good description of the stability of a ship in still water, such as the initial metacentric distance (GM); the largest steady heeling force that the vessel can withstand without capsizing (maximum GZ); range of stability; and angle of deck edge immersion. However, large-amplitude ship motions are essentially transient due to the sudden appearance of waves and a gust of wind. Further, the ship capsizing, resulting from these nonlinear motions, is a dynamic process, the transient condition is therefore a much more useful measure of capsizing.

[13-15] first introduced the concept of "safe basin" to the study of the nonlinear ship rolling motion and capsizing. For a ship in still water experiencing a single-degree-of-freedom (1-DOF) roll motion due to initial disturbance, plotting the evolving solution of the 1-DOF dynamic system as a trajectory in phase space (with normalised roll angle and roll angular velocity as x and y axes respectively) rather than as a time history, [14,15] obtained a trajectory spiral into the origin as the ship comes to rest. Stationary steady solutions are represented in phase space by points, while periodic solutions appear as closed curves, such as the case of a ship in waves. Those stable solutions are called attractors, while the unstable solutions are called repellers. The combination of the domains of all attractors is termed the safe basin [9].

Marshfield [5] demonstrated the nonlinear character of the frequency response curve and the existence of bi-stability within a certain range around resonance through "Admiralty model tests". By applying the nonlinear dynamic system theory on the ship-capsize problem, [9] and [16] considered the capsizing process as dynamically equivalent to the escape of a ball rolling in a potential well, i.e. a transient phenomenon. The significance of the new method of quantifying stability of a ship in waves is that the use of the transient capsizing diagram to assess the ship hull's capsizability, and the demonstration of considerable impact of bias on the maximum wave slope at which capsizing is still resisted. [3] extended the nonlinear dynamic system theory to the study of 1-DOF nonlinear rolling motion and capsizing of biased ships in random beam seas. Compared to the inertia effects and hydrostatic righting moments, the relatively small damping and wave excitation moments were treated as perturbations. Assuming an unperturbed system model, safe and unsafe areas were defined in the phase plane to distinguish the qualitatively different ship motions of capsizing and non-capsizing. Capsizing events were represented by solutions passing out of the safe region.

Finally, they presented the quantitative description of the influence of bias on the probability of capsizing in random beam seas, and concluded that the widening of the dangerous significant frequency range when bias is presented.

In this paper, a current-in-use cargo ship is used for the study of safe basin erosion. The nonlinear damping, which is very important to ship roll motion in waves, is obtained by an experiment of the ship model rolling in waves in a wave tank. Other coefficients in the roll motion equation of the ship in waves are obtained through theoretical methods. The safe basins with and without heel angle are discussed, and the safe basin erosions caused by the exciting wave spectrum and the pulse wind spectrum are investigated by using a quantitative method.

Theoretical Formulation

A typical roll motion with single degree of freedom can be described as

$$(I + \Delta I(\omega))\ddot{\theta} + B(\omega)\dot{\theta} + C\theta = F_{wave}(t) + F_{wind}(t), \quad (1)$$

where θ is the roll angle, $\dot{\theta}$ and $\ddot{\theta}$ are the first and second derivatives with respect to time, I is the total moment of inertia in roll, $\Delta I(\omega)$ is the roll added mass coefficient, $B(\omega)\dot{\theta}$ is the nonlinear damping moment, $C\theta$ is the nonlinear restoring moment, $F_{wave}(t)$ is the wave exciting moment, and $F_{wind}(t)$ is the wind exciting moment. Various expressions of damping and restoring terms were used to simulate the nonlinear characteristics of roll motion. The commonly used representations are:

$$B(\omega)\dot{\theta} = B_L(\omega)\dot{\theta} + B_N(\omega)\dot{\theta}|\dot{\theta}|, \quad (2)$$

$$C\theta = C_0 + C_1\theta + C_3\theta^3, \quad (3)$$

where B_L and B_N are the linear and nonlinear damping coefficients respectively, C_1 and C_3 are the linear and third-order restoring force coefficients, and C_0 is the bias moment which can arise due to wind, cargo, ship damage or the pull of a fishing net.

Eq. 1 is a frequency domain description since $\Delta I(\omega)$ and $B(\omega)$ are frequency-dependent due to the presence of the free surface. Following [7], the time-domain ship rolling motion equation can be written as:

$$(I + \Delta I(\infty))\ddot{\theta} + \int_0^\infty K(t-\tau)\dot{\theta}(\tau)d\tau + B_N\dot{\theta}|\dot{\theta}| + C_0 + C_1\theta + C_3\theta^3 = F_{wave}(t) + F_{wind}(t) \quad (4)$$

where $\Delta I(\infty)$ is the hydrodynamic added mass coefficient evaluated at the infinite frequency limit; $K(t)$ is the hydrodynamic rolling moment due to impulse roll velocity expressed as Eq. 5; and its integral is usually called the memory function, as it represents how roll-radiation moments depend on the history of rolling velocity.

$$K(t) = \frac{2}{\pi} \int_0^\infty (B_L(\omega) - B(\infty)) \cos(\omega t) d\omega. \quad (5)$$

Following [17], the wave exciting moment $F_{wave}(t)$ can be expressed by

$$F_{wave}(t) = \int_0^\infty \frac{F_{wave}(\omega)}{\zeta_0} \cos(\omega t + \varepsilon(\omega)) \sqrt{2S_\zeta(\omega)} d\omega, \quad (6)$$

where $F_{wave}(\omega)/\varepsilon_0$ is the response function of wave exciting moment in frequency domain; $\varepsilon(\omega)$ is the response function of the phase difference in frequency domain represented by a random value between 0 and 2π ; and $S_\varepsilon(\omega)$ is the wave elevation spectrum represented by ITTC two-parameter formula:

$$S_\varepsilon(\omega) = \frac{A}{\omega^5} \exp[-B/\omega^4], \quad (7)$$

where $A = 173H_{1/3}^2/T_z^4$, $B = 691/T_z^4$, $H_{1/3}$ is the significant wave height and T_z is the zero up-crossing wave period.

Following [1], the wind exciting moment $F_{wind}(t)$ can be expressed as:

$$F_{wind}(t) = \frac{1}{2} C_m \rho_a A_w z_a u^2(t), \quad (10)$$

where C_m is the wind moment coefficient; ρ_a is the density of air; A_w is the wind area; z_a is the height of the wind area centre; and $u(t)$ is the velocity of wind. In order to determine the safe basin erosion caused by the wind, the pulse wind spectrum different to that of [1] is adopted, and can be described by a Fourier series:

$$u(t) = u_0 + \sum_{i=1}^{\infty} u_i \cos(\omega_i t + \varepsilon_i), \quad (11)$$

where u_0 is the average velocity of wind; ω_i is the pulse frequency of wind velocity; ε_i is the phase difference of wind velocity; and u_i is the turbulent velocity of wind expressed as:

$$u_i = \sqrt{2S_u(\omega)d\omega}, \quad (12)$$

where the wind velocity spectrum can be represented by Von Karman spectrum [11],

$$S_u(\omega) = \frac{4\bar{u}^2 L_x^u}{\bar{U} [1 + (2c\omega(L_x^u/\bar{U}))^2]^{5/6}}, \quad (13)$$

where \bar{U} is the longitudinal mean wind speed; ω is the frequency of pulse wind; L_x^u is the longitudinal turbulence integral length scale of longitudinal turbulence; \bar{u}^2 is the variance of longitudinal turbulent velocity; and c is a constant that is the function of height of observation site and its surrounding terrain.

Since the general solution for nonlinear ordinary differential equation with 1-DOF describing roll motion of a ship in waves is unknown, the solution of Eq. 4 will be obtained by numerical simulation. The phase space consists of roll angle θ (-1.5~1.5) and roll velocity $\dot{\theta}$ (-0.31~0.31), and is divided into 600×620 small areas. Eq. 4 with initial condition including the values of each small area is solved by using the Adams fourth-order trial and error method. If the solution can be obtained, the small area is called the domain of safe abstract marked black. The safe basin is obtained by the combination of the domains of all the safe attractors.

Parameters and coefficients of the ship

The data of a current-in-use cargo ship introduced in our study are given in Table 1. The GZ curve of the ship is shown in Fig. 1. The linear and third-order restoring moment coefficients are obtained by the fitting of the GZ curve, $C_1^* = 0.56725$ and $C_3^* = -0.47992605$.

Then the linear and third-order restoring force coefficients are:

$$C_1 = \Delta g C_1^*, \text{ and } C_3 = \Delta g C_3^*.$$

The linear damping is obtained by numerical computation using 3D Source Distribution Method, while nonlinear damping is

obtained by an experiment of the model ship rolling in irregular waves. The value of nonlinear damping B_N ($= 2.502 \times 10^6 \text{ kg} \cdot \text{m}^2$), is finally obtained from roll time record in irregular waves using Random Decrement Technique. For details of the obtaining of nonlinear damping in an experiment, readers can refer to [4].

Length overall	105.9 m	L _p	99 m	Displacement	6.2 x 10 ⁶ kg
Mean Draft	5.55 m	Inertial Radius of Roll	0.35 m	Centre of Gravity above Baseline	6.715 m
Breadth	16.0 m	Depth	9 m	Natural Period of Roll	23.55 s

Table 1. Principle dimensions of the cargo ship.

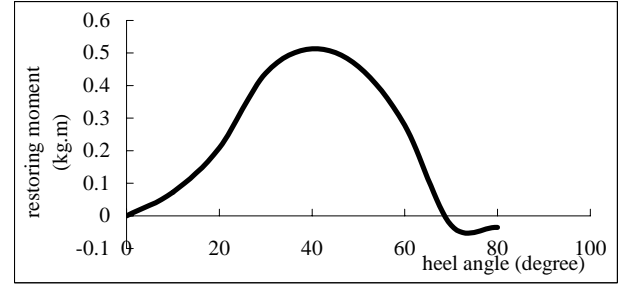


Fig. 1 GZ curve of the ship.

Results and discussion

Effects of heel angle

The safe basins with different heel angles without wind and waves are shown in Fig. 2- Fig. 4. The intersection of the top line and bottom line is called a saddle, which is the position where the safe basin begins to disappear. The values of saddles with different initial heel angle δ are shown in Table 2. Several significant differences between safe basins with or without heel angle can be observed from the figures: 1) The safe basin without heel angle, which is symmetric to x-axis and y-axis, is composed of a top and bottom curve, while the safe basin which is asymmetric to y-axis is closed by a curve when the heel angle appears; 2) The value of the left saddle is different from the value of the right saddle when the heel angle appears; 3) The area of safe basin decreases as the heel angle increases; 4) no safe basin erosion occurs if wind and waves are not considered.

Heel angle (rad.)	Values of left saddle (rad.)	Values of right saddle (rad.)
0	-1.0871	1.0871
0.01	-1.06756	0.9336
0.08	-1.03998	0.60985

Table 2 Values of saddle with different hell angles.

Effects of waves

Fig. 5 and Fig. 6 are the safe basins in [10] and the present study respectively, using wave slope spectrum for the excitation parameters $a/\omega_0^2 = 0.03, \omega_N/\omega_0 = 0.9$ (equal to excitation parameters $H_{1/3} = 6 \text{ m}, \bar{T} = 10 \text{ s}$). However, the response function of the exciting moment in [10] is a sinusoidal response function, while the response function in the present study is a response curve obtained from theoretical calculation. As can be seen from the figures, excellent agreement is obtained, indicating the feasibility of present method. The safe basin using the ITTC spectrum with the same excitation parameter $H_{1/3} = 6 \text{ m}, \bar{T} = 10 \text{ s}$ is shown in Fig. 7. The quantitative results are obtained by an introduction of safe basin ratio A_s , a value of computational area divided by the safe basin area. The values of A_s in Fig. 6 and Fig. 7 are 0.548 and 0.352 respectively,

demonstrating the significant impact of the selection of wave spectrum on safe basin erosion. The adoption of the wave slope spectrum results in the evaluation of a larger safe basin area.

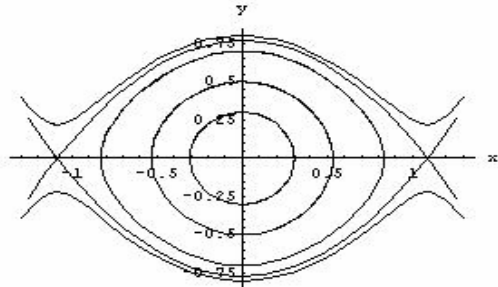


Fig. 2 Safe basin without wind and waves ($\delta = 0$)

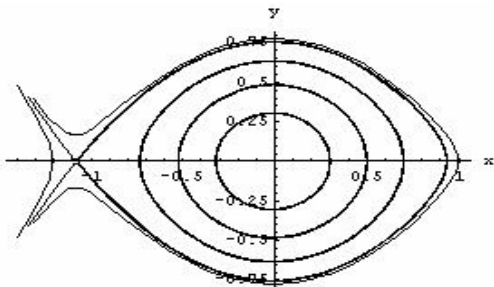


Fig. 3 Safe basin without wind and waves ($\delta = 0.01$)

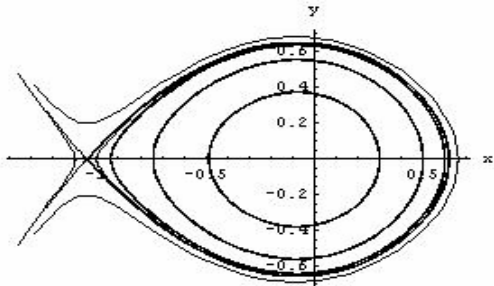


Fig. 4 Safe basin without wind and waves ($\delta = 0.08$)

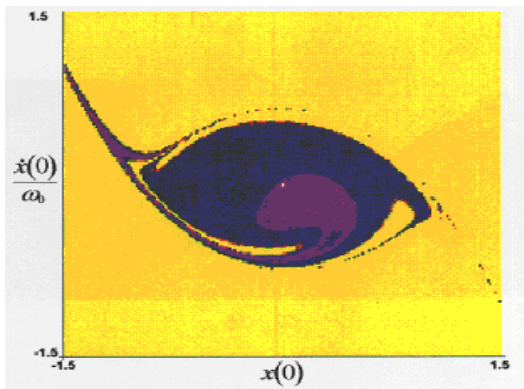


Fig. 5 Safe basin in waves using wave slope spectrum, $a / \omega_0^2 = 0.03, \omega_N / \omega_0 = 0.9$.

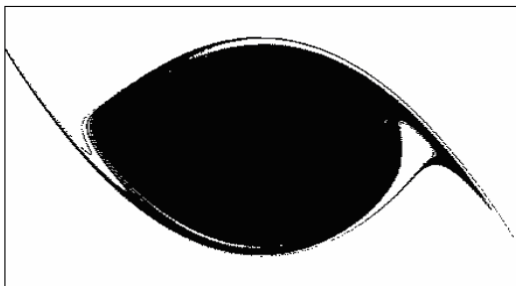


Fig. 6 Safe basin in waves using wave slope spectrum, $H_{1/3} = 6\text{m}, \bar{T} = 10 \text{ s}$.

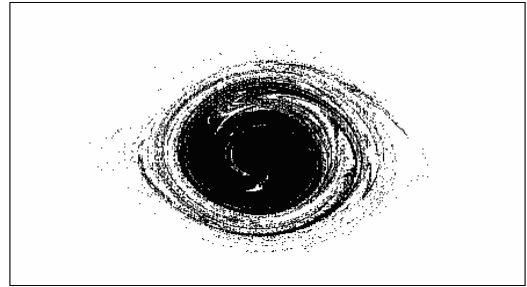


Fig. 7 Safe basin in waves using ITTC spectrum ($H_{1/3} = 6\text{m}, \bar{T} = 10 \text{ s}$).

Fig. 8 and Fig. 9 show safe basins obtained using ITTC spectrum with different $H_{1/3}$ and same \bar{T} . Fig. 10 is a safe basin obtained using ITTC spectrum with excitation parameters $H_{1/3} = 6 \text{ m}, \bar{T} = 6 \text{ s}$ (the same $H_{1/3}$ as in Fig. 7). As can be seen, the higher the wave height $H_{1/3}$, the smaller the safe basin area. However, it appears that the effect of a wave period on the safe basin area is small. This is because the much longer natural roll period of the ship compared to the wave periods.

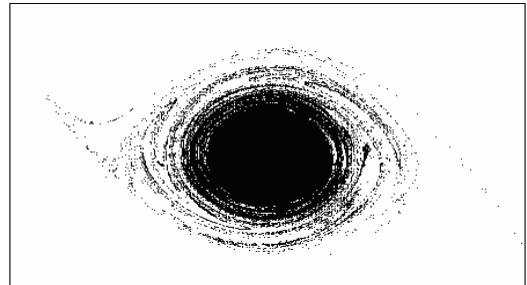


Fig. 8 Safe basin in waves using ITTC spectrum ($H_{1/3} = 5\text{m}, \bar{T} = 8 \text{ s}$).

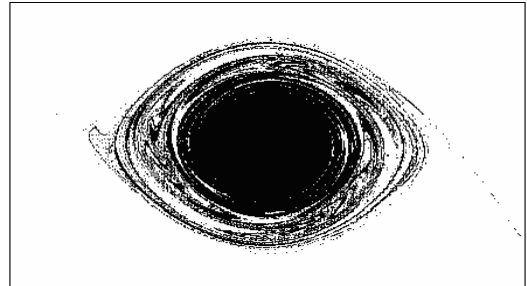


Fig. 9 Safe basin in waves using ITTC spectrum ($H_{1/3} = 3\text{m}, \bar{T} = 8 \text{ s}$).

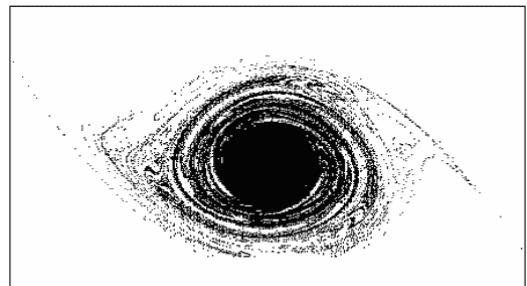


Fig. 10 Safe basin in waves using ITTC spectrum ($H_{1/3} = 6\text{m}, \bar{T} = 6 \text{ s}$).

There is a significant difference in the shape of safe basin in waves in comparison with the safe basin in calm water without wind. The two sides of the boundary have extended outside, and even the unsafe attractors appear inside the safe basin, i.e. the safe basin erosion occurs. As can be seen, the ship is more dangerous under the higher wave height $H_{1/3}$, as the safe basin erosion area is larger.

Effects of wind and waves

The velocity and turbulence statistics at the north-eastern coast of Taiwan under high-wind condition by [11], is selected as the environmental condition for the present study. The different wind parameters, also used by [2], are shown in Table 3.

When wind is considered, safe basin erosion occurs (see Fig. 11 for $\bar{U} = 18.78$ m/s). Fig. 12 is the safe basin obtained using ITTC spectrum with wave excitation parameter $H_{1/3} = 5$ m, $\bar{T} = 8$ s and wind parameter $\bar{U} = 15.58$ m/s. Compared to the safe basin in Fig. 8, it can be seen that their shapes are almost identical. However, the different safe basin ratios A_s (0.1410 in Fig. 8 and 0.1381 in Fig. 12) indicate that the effect of wind on the safe basin is not negligible.

Conclusions

Ship capsizing has been studied using safe basin theory. The effects of initial heel angle, waves and winds on safe basin erosion have been discussed. The following conclusions can be drawn from the present study:

- The area of the safe basin is dependent on the heel angle. The larger the heel angle, the smaller the area of the safe basin. However, no safe basin erosion occurs if the ship is in calm water without wind.
- The wave exciting spectrum is found to have a significant effect on the safe basin erosion. The safe basin area is unreasonably large if the ideal wave spectrum is used.
- The wave height has a greater impact on safe basin erosion than the wave period. The pulse wind is also found to cause safe basin erosion. The random properties of wind and waves should be considered in the investigation of safe basin erosion.

Acknowledgments

This research project was sponsored by the National Natural Science Foundation of China, Grant No.10072021.

References

- [1] Belenky, V.L., Degtyarev, A.B. & Boukhanovsky, A.V., Probabilistic qualities of nonlinear stochastic rolling, *Ocean Engineering*, **25**(1), 1998, 1-25.
- [2] Bhattacharyya, R., *Dynamics of marine vehicles*, New York, Wiley & Sons Inc., 1978.
- [3] Jiang, B.Y.C., Troesch, A.W. and Shaw, S.W., Highly nonlinear rolling motion of biased ships in random beam sea, *J. of Ship Res.*, **40**(2), 1996, 125-135.
- [4] Li, Y.L. and Wu, X.R., Experimental Determination of Nonlinear roll Damping: a Technique for Data Processing (In Chinese), *J. of South China University of Tech.*, **30**(2), 2002, 79-82.
- [5] Marshfield, W.B., AMTE-NMI capsizing experiments, *Admiralty Research Establishment*, Haslar Gosport Hants, Report TM78011, 1978.
- [6] Odabashi, A.Y., Methods of analysing nonlinear ship oscillations and stability, Department of Shipbuilding and Naval Architecture, University of Strathclyde, Report No 08/73, 1973.
- [7] Ogilvie, T.F., Recent progress toward the understanding and prediction of ship motions, *Proc. 5th Symp. on Naval Hydrodynamics*, 1964, 3-80.
- [8] Oh, I., Nayfeh, A.H. and Mook, D., Theoretical and experimental study of the nonlinearly coupled heave, pitch and roll motions of a ship in longitudinal waves, *Proc. 19th Symp. on Naval Hydrodynamics*, **2**, 1992, 71-89.
- [9] Rainey, R.C.T. and Thompson, J.M.T., The Transient Capsizing Diagram - A New Method of Quantifying Stability in Waves, *J. of Ship Res.*, **35**(1), 1991, 58-62.

$H_{1/3}$ (m)	\bar{T} (s)	\bar{U} (m/s)	L_x^u	$\overline{u^2}$	C
3.0	6.0	12.35	-	-	4.023
5.0	8.0	15.58	40.8	9.516	4.023

Table 3 Wind conditions.

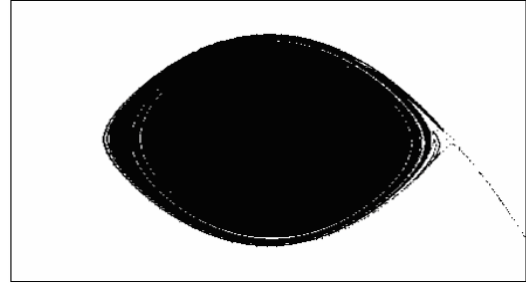


Fig. 11 Safe basin in wind ($\bar{U} = 18.78$ m/s).

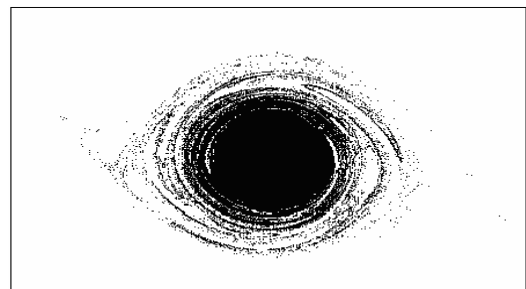


Fig. 12 Safe basin in wind and waves using ITTC spectrum ($H_{1/3} = 5$ m, $\bar{T} = 8$ s, $\bar{U} = 15.58$ m/s).

- [10] Senjanvic, I. and Fan, Y., Numerical simulation of a ship capsizing in irregular waves, *Chaos, Solitons & Fractals*, **5**(5), 1995, 727-737.
- [11] Shiau, B.S., Velocity spectra and turbulence statistics at the northeastern coast of Taiwan under high-wind conditions, *J. of Wind Engineering and Industrial Aerodynamics*, **88**, 2000, 139-151.
- [12] Spyrou, K.J. and Thompson, J.M.T., The nonlinear dynamics of ship motions: a field overview and some recent developments, *Phil. Trans. Roy. Soc. Lond. A* **358**, 2000, 1735-1760.
- [13] Thompson, J.M.T. and Stewart, H.B., *Nonlinear dynamics and chaos*, New York, John Wiley & Sons Inc., 1987.
- [14] Thompson, J.M.T., Loss of engineering integrity due to the erosion of absolute and transient basin boundaries, *Proc. of IUTAM Symp. On the Nonlinear Dynamics in Engineering Systems*, 1989, 313-320.
- [15] Thompson, J.M.T., Transient basins: a new tool for designing ships against capsizing, *Proc. of IUTAM Symp. on the Dynamics of Marine Vehicles & Structures in Waves*, 1990, 325-331.
- [16] Thompson, J.M.T. and Soliman, M.S., Fractal control boundaries of driven oscillators and their relevance to safe engineering design, *Proc. of The Royal Society, London*, **A 428**, 1990, 1-13.
- [17] Van Oortmerssen, G., *The motions of a moored ship in waves*, Thesis, MARIN Publications No. 510, 1976.
- [18] Wellicome, J.F., An analytical study of the mechanism of capsizing, *Proc. 1st International Conf. on Stability of Ships and Ocean Vehicles*, University of Strathclyde, 1975.
- [19] Wright, J.H.G. and Marshfield, W.B., Ship roll response and capsizing behaviour in beam seas, *Transactions RINA*, **122**, 1980, 129-148.